Synthesis, structural characterization and *in vitro* cytotoxicity of new Au(III) and Au(I) complexes with thioamides†

K. N. Kouroulis,[a] S. K. Hadjikakou,*[a] N. Kourkoumelis,[b] M. Kubicki,[c] L. Male,[d] M. Hursthouse,[d] S. Skoulika,[e] A. K. Metsios,[f] V. Y. Tyurin,[g] A. V. Dolganov,[g] E. R. Milaeva[g] and N. Hadjiliadis*[a]

Received 14th May 2009, Accepted 18th September 2009
First published as an Advance Article on the web 13th October 2009
DOI: 10.1039/b909587j

The reactions of tetrachloroauric(III) acid ($HAuCl_4$) with the thioamides; 2-mercapto-benzothiazole (mbztH) and 5-ethoxy-2-mercapto-benzimidazole (EtmbzimH) lead to the desulfuration of the ligands and the formation of the ionic complexes {$[AuCl_4]^-[bztH_2]^+$} (**1**), and {$[AuCl_4]^-[EtbzimH_2]^+(H_2O)$} (**2**) (where $bztH_2^+$ and $EtbzimH_2^+$ are the desulfurated cations of the starting ligands). The reaction of $HAuCl_4$ with 2-mercapto-nicotinic acid ($mnaH_2$), however results in the formation of 2-sulfonate-nicotininc acid ($C_6H_5NO_5S$) (**3**) with the simultaneous oxidation of the sulfur atom. On the other hand, the reactions of the gold(I) complex [Au(tpp)Cl] (**4**) (tpp = triphenylphosphine (Ph_3P)) with the thioamides; 2-mercapto-thiazolidine (mtzdH), 2-mercapto-benzothiazole (mbztH) and 5-chloro-2-mercapto-benzothiazole (ClmbztH) in the presence of potassium hydroxide resulted in the formation of the gold(I) complexes of formulae [Au(tpp)(mtzd)] (**5**), [Au(tpp)(mbzt)] (**6**) and [Au(tpp)(Clmbzt)] (**7**) without ligand desulfuration. All complexes have been characterized by elemental analysis, FT-IR, far-FT-IR,^{1}H-NMR, spectroscopic techniques and X-Ray crystallography. The electrochemical behavior of **1**, **2** and **4-7** complexes and the ligands EtmbzimH, mbztH and $mnaH_2$ was also studied in acetonitrile and DMF using cyclic voltammetry. The results are in support of a mechanism of desulfuration of the ligands by Au(III), involving a first oxidation of S to $-SO_3^-$, followed by a C-S bond cleavage. This is also supported by PM6 calculations of bond dissociation energies of the various compounds involved. Complexes **1**, **2** and **4-7** were tested for *in vitro* cytotoxicity against leiomyosarcoma cells and the results are discussed in relation with the geometry of the complexes and compared with those of cisplatin and other metals. Complexes **1** and **5** showed higher activity than that of cisplatin, while $HAuCl_4$ was inactive against sarcoma cells.

Introduction

Chrysotherapy, is the use of gold compounds in medicine with many applications.[1-3] Gold thiolates are used clinically against rheumatoid arthritis.[1-3] Recently, many gold(III) and gold(I) compounds were tested for their antitumor activity against various cancerous cell lines[4] and the results have been reviewed by Tiekink.[4a] A commonly cited reason for the anti-tumor investigation of gold compounds relates to the square-planar geometry, also found for platinum in cisplatin, since gold(III) is isoelectronic with platinum(II) and forms similar square-planar complexes.[4] Given the generally reducing mammalian environment, compounds containing gold(III) may be expected to be reduced *in vivo* to gold(I) and this led to the investigation of possible antitumor properties of gold(I) compounds as well.[4] However, appropriate selection of the ligand donor set (*e.g.* N or O) can serve to stabilize gold(III) and consequently there is a rich literature of anti-tumour/cytotoxicity investigations of such species.[4a]

In the course of our studies on metalotherapeutics we synthesized and structurally characterized new gold(III) complexes with the thioamides 2-mercapto-benzothiazole (mbztH) and 5-ethoxy-2-mercapto-benzimidazole (EtmbzimH) of formulae {$[AuCl_4]^-[bztH_2]^+$} (**1**), and {$[AuCl_4]^-[EtbzimH_2]^+(H_2O)$} (**2**) (where $bztH_2^+$ and $EtbzimH_2^+$ are the desulfurated cations of the starting ligands) (Scheme 1). Also for gold(I) mixed ligand complexes of [Au(tpp)Cl] (**4**) with the thioamides 2-mercapto-thiazolidine (mtzdH), 2-mercapto-benzothiazole (mbztH) and 5-chloro-2-mercapto-benzothiazole (ClmbztH) and tri-phenyl-phosphine (tpp) of formulae [Au(tpp)(mtzd)] (**5**), [Au(tpp)(mbzt)] (**6**) and [Au(tpp)(Clmbzt)] (**7**) (Scheme 1). Moreover in the reaction of $HAuCl_4$ with 2-mercapto-nicotinic acid ($mnaH_2$) the ligand is oxidized to 2-sulfonate-nicotininc acid ($C_6H_5NO_5S$) (**3**).

[a]*Inorganic and Analytical Chemistry, Department of Chemistry, University of Ioannina, 45110, Ioannina, Greece. E-mail: nhadjis@uoi.gr, shadjika@uoi.gr; Fax: +30-26510-08786; Tel: +30-26510-08420; Tel: +30-26510-08374*
[b]*Medical Physics Laboratory, Medical School, University of Ioannina, Greece*
[c]*Department of Chemistry, A. Mickiewicz, University, ul. Grunwaldzka 6, 60-780, Poznan, Poland*
[d]*Department of Chemistry, University of Southampton, Highfield, Southampton, UK SO17 1BJ*
[e]*Section of Physical Chemistry, Department of Chemistry, University of Ioannina, 45110, Ioannina, Greece*
[f]*Department of Experimental Physiology, Medical School, University of Ioannina, 45110, Ioannina, Greece*
[g]*Chemistry Department, M.V. Lomonosov Moscow State University, Leninskie Gory, 119992, Moscow, Russia*
† CCDC reference numbers 732324 (**1**), 732325 (**2**), 733450 (**3**), 732369 (**6**) and 732368 (**7**). For crystallographic data in CIF or other electronic format see DOI: 10.1039/b909587j

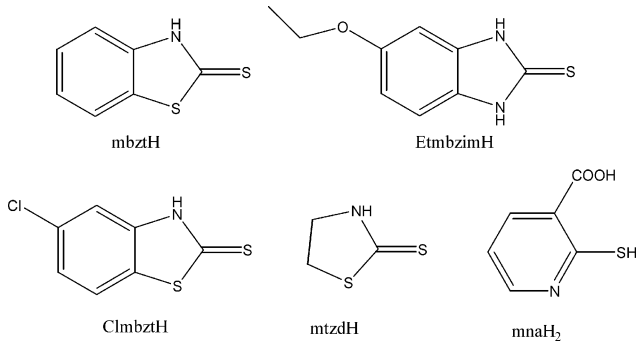

Scheme 1 The ligands used in this study.

The use of $AuCl_4^-$ as a counter ion in complexes **1** and **2** and the isolation of 2-sulfonate-nicotinic acid ($C_6H_5NO_5S$; (**3**)), strongly indicates that $AuCl_4^-$ acts rather as a catalyst, while the oxidation is taking place with atmospheric O_2 as it was also found in the case of the oxidation of thioethers by this anion.[5] Electrochemical and computational studies on the other hand, strongly indicate that oxidation of the ligands at S, takes place prior of the breaking of the C-S bonds in the final products. Based on these results, a possible mechanism of the reaction taking place was proposed.

The electrochemical properties of gold(III) complexes with N,N-dimethyldithiocarbamate (DMDT) and ethylsarcosinedithiocarbamate (ESDT) in acetonitrile have been previously investigated by cyclic voltammetry.[4b] The reduction of the gold(III) compounds followed two separated Au(III)/Au(II) and Au(II)/Au(I) steps leading to the formation of a dimeric gold(II) species with bridging chlorine atoms.[4b] This is different than the behavior of the complexes in the present study, which involves the Au(III)/Au(I) and Au(I)/Au(0) reduction processes.

The electrochemical behavior of the free ligands EtmbzimH, mbztH and $mnaH_2$ was also evaluated in CH_3CN and DMF solutions. The results showed that the easiness of ligand's oxidation changes in the order: EtmbzimH > mbztH > $mnaH_2$. The desulfurated product of $mnaH_2$ by means of the controlled potential electrolyses which was performed in acetonitrile were achieved at the first anodic wave potential of E = 1.3 V. This support the assumption that the oxidation of $mnaH_2$ ligand also proceeds the desulfuration step.

Finally, the *in vitro* cytotoxicity of complexes **1-2** and **4-7** and $HAuCl_4$ against leiomyosarcoma cells were also evaluated and the results were compared with analogous Sn(IV), Ag(I), Sb(III) complexes, reported by our group earlier[6] and cisplatin.

Results and discussion

General aspects

Tetrachloroauric(III) acid ($HAuCl_4$) solution was prepared according to the literature by dissolving Au foil into a mixture of concentrated hydrochloric acid and nitric acid 4:1.[7] Complexes **1** and **2** were obtained by reacting 1 mmol of the appropriate thioamides 2-mercapto-benzothiazole (mbztH) and 5-ethoxy-2-mercapto-benzimidazole (EtmbzimH) with 0.5 mmol of $HAuCl_4$ solution in methanol/acetonitrile) under reflux for 3 h (Scheme 2, reaction I). The reaction of 0.5 mmol $HAuCl_4$ with 1 mmol 2-mercapto-nicotinic acid ($mnaH_2$) on the other hand, treated with an equimolar amount of KOH, resulted in the formation of 2-sulfonate-nicotininc acid ($C_6H_5NO_5S$) (**3**) with simultaneous oxidation of the sulfur atom (Scheme 2, reaction II). Au(I) complexes **5**, **6** and **7** were synthesized by reacting 1 mmol of [Au(tpp)Cl][8] (**4**) with 1 mmol of the appropriate thioamide 2-mercapto-thiazolidine (mtzdH), 2-mercapto-benzothiazole (mbztH) or 5-chloro-2-mercapto-benzothiazole (ClmbztH) in the presence of an equimolar amount of KOH, in methanol/water solution (Scheme 2, reaction III).

All complexes are air stable powders. Crystals of compounds **1**, **2** and **3**, suitable for X-ray analysis, were obtained by slow evaporation of a methanol/acetonitrile (1:1) solution. Crystals of **5**, **6** and **7** were grown from a dichloromethane/toluene (1:1) solution.

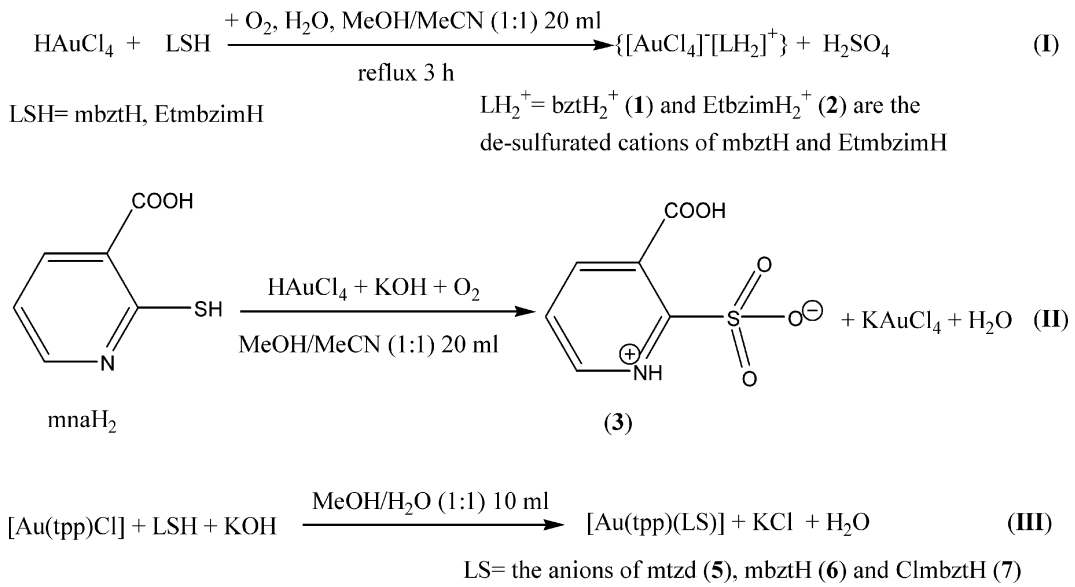

Scheme 2

The crystal structures of **4** and **5** were also re-determined here and found identical to the ones previously reported.[9-12]

Vibrational spectroscopy

The infrared spectra of complexes **1** and **2** show strong vibrational bands at 3211 (**1**) and 3279 (**2**) cm^{-1}, respectively, which are assigned to ν(N-H) stretching vibrations, while no such bands were observed in the spectra of complexes **5**, **6** and **7** indicating the de-protonation of their ligands. The corresponding ν(N-H) vibration bands are observed at 3111 cm^{-1} (mbztH), 3084 cm^{-1} (EtmbzimH), 3107 cm^{-1} (ClmbztH) and at 3133 cm^{-1} (mtzdH).[13-19] The vibrational thioamide bands I and II, appear at 1446-1479 cm^{-1} and 1182-1309 cm^{-1} respectively in the IR spectra of complexes **1**, **2**, **5**, **6** and **7** shifted to lower wavenumbers as compared with the corresponding vibrational bands of the free ligands mbztH, EtmbzimH, mtzdH and ClbztH shown at 1496-1514 cm^{-1} and 1248-1319 cm^{-1} respectively.[16-19] Thioamide bands III-IV, observed at 995-1173 cm^{-1} and at 652-811 cm^{-1}, in the spectra of the free ligands,[16-19] appear at 1024-1075 cm^{-1} and 634-789 cm^{-1} respectively in the spectra of complexes **5**, **6** and **7**. The absence of the thioamide bands in the spectra of complexes **1** and **2** indicate the desulfuration of the 2-mercapto-benzothiazole (mbztH) or 5-ethoxy-2-mercapto-benzimidazole (EtmbzimH) ligands upon their reaction with Au(III).

The new bands at 365 and 360 cm^{-1} in the far-IR spectra of complexes **1** and **2** have been assigned to the ν(Au-Cl) vibrations,[20-22] while bands appearing at 279 and 180 (**5**), 280 and 179 (**6**) and 279 and 171 (**7**) cm^{-1} in the far-IR spectra of complexes **5-7** are attributed to the ν(Au-S) and ν(Au-P) vibrations.[20-22]

Crystal and molecular structures of $\{[AuCl_4]^-[bztH_2]^+\}$ (1), $\{[AuCl_4]^-[EtbzimH_2]^+(H_2O)\}$ (2), the 2-sulfonate-nicotininc acid (3), [Au(tpp)(mbzt)] (6) and [Au(tpp)(Clmbzt)] (7)

The structures of compounds **1-3** and **6**, **7** were solved by X-ray diffraction at 120(2) K for **1** and **2**, and at r.t. (293(2) K) for **3** and **7**.

ORTEP diagrams of compounds **1-3** and **6-7** are shown in Figs. 1-5. Selected bond distances and angles are given in Table 1.

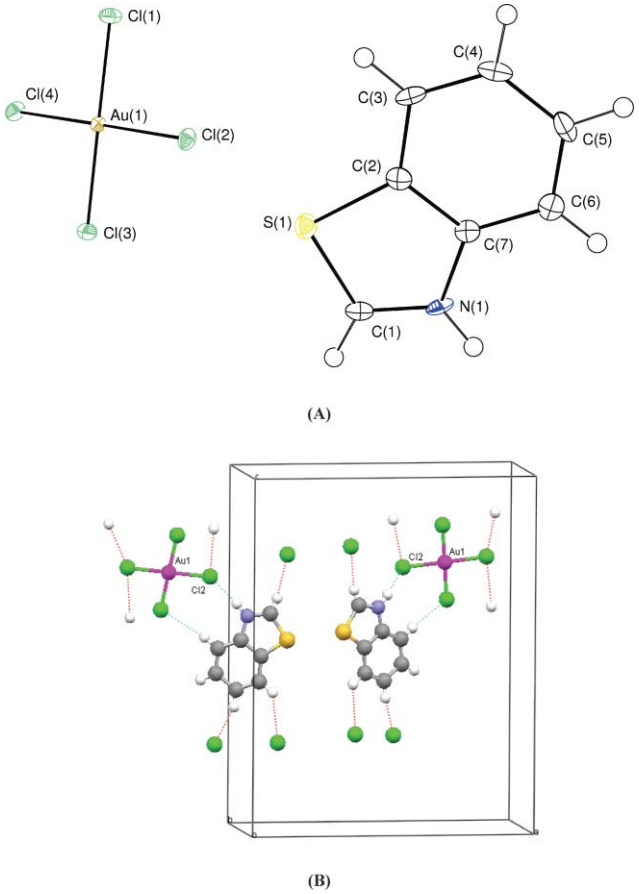

Fig. 1 (A) Anisotropic ellipsoid representation of the building block of complex **1**. The ellipsoids are drawn at 50% probability level. (B) Strong hydrogen bonding interactions.

Complexes **1** and **2** are ionic salts containing an $[AuCl_4^-]$ counter anion neutralized by a protonated fragment of the

Table 1 Selected bond lengths (Å) and angles (deg) of compounds **1-3** and **6-7**

Complex **1**		Complex **2**		Compound **3**		Complex **6**		Complex **7**	
(a) bond lengths		*(a) bond lengths*		*(a) bond lengths*		*(a) bond lengths*		*(a) bond lengths*	
Au1 Cl4	2.2808(13)	Au1 Cl2i	2.2765(16)	S1-O1	1.444(3)	Au1-S22	2.2960(13)	Au1-S22	2.296(3)
Au1 Cl3	2.2816(12)	Au1 Cl2	2.2765(16)	S1-O2	1.439(3)	Au1-P1	2.2559(11)	Au1-P1	2.259(3)
Au1 Cl2	2.2867(13)	Au1 Cl1i	2.2799(16)	S1-O3	1.437(3)	S22-C22	1.743(5)	S22-C22	1.736(14)
Au1 Cl1	2.2884(12)	Au1 Cl1	2.2799(16)	S1-C1	1.808(3)	N23-C22	1.298(6)	N23-C22	1.275(16)
C1 N1	1.308(7)	C1 N2	1.322(7)	N2-C1	1.343(4)	N23-C23A	1.402(6)	N23-C23A	1.393(16)
C7 N1	1.398(6)	C3 N2	1.389(6)	N2-C3	1.335(4)				
C1 S1	1.684(5)	C2 N1	1.388(6)	C1-C6	1.390(4)				
		C1 N1	1.333(6)						
(b) angles		*(b) angles*		*(b) angles*		*(b) angles*		*(b) angles*	
Cl4 Au1 Cl3	90.31(4)	Cl2i Au1 Cl2	180.0	S1-C1-C6	126.8(3)	S22-Au1-P1	176.25(5)	S22-Au1-P1	176.11(9)
Cl4 Au1 Cl2	178.81(4)	Cl2i Au1 Cl1i	90.0	S1-C1-N2	114.7(2)	S21-C22-S22	117.3(3)	S21-C22-S22	121.5(7)
Cl3 Au1 Cl2	89.14(4)	Cl2 Au1 Cl1i	90.0	N2-C1-C6	118.4(3)	S21-C22-N23	115.9(4)	S21-C22-N23	115.8(11)
Cl4 Au1 Cl1	90.45(5)	Cl2i Au1 Cl1	90.0			S22-C22-N23	126.6(4)		
Cl3 Au1 Cl1	179.20(5)	Cl2 Au1 Cl1	90.0						
Cl2 Au1 Cl1	90.11(5)	Cl1i Au1 Cl1	180.00(3)						
N1 C1 S1	114.4(4)	N2 C1 N1	110.4(4)						

Symmetry transformations used to generate equivalent atoms: (i) –x+1,–y,–z+1

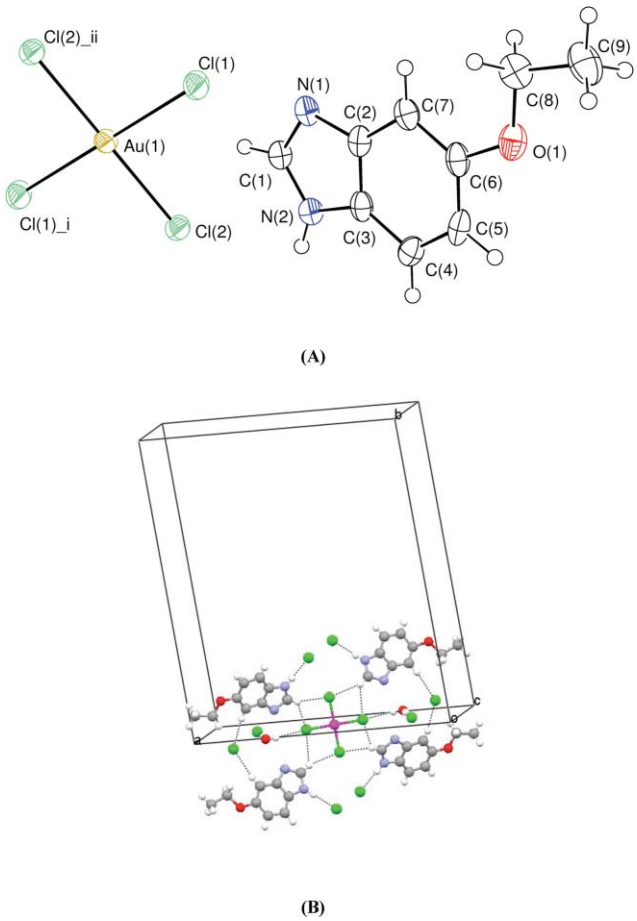

Fig. 2 (A) Anisotropic ellipsoid representation of the building block of complex **2**. The ellipsoids are drawn at 50% probability level. The chloride and oxonium ions and water molecules are not shown for clarity. (B) Strong hydrogen bonding interactions.

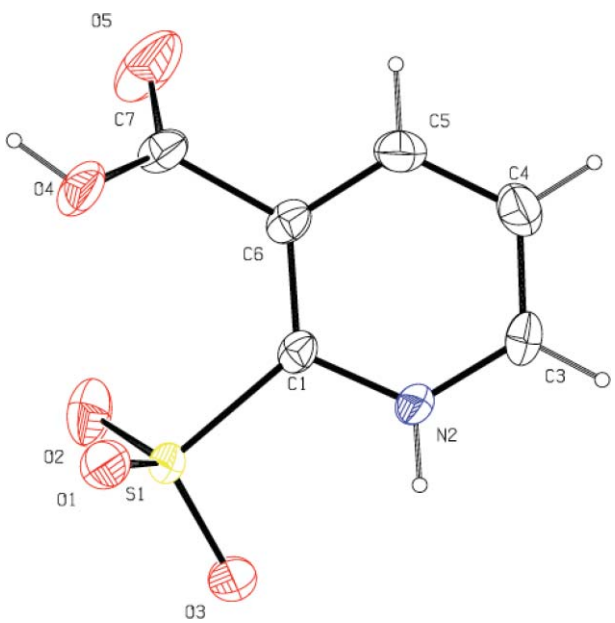

Fig. 3 Anisotropic ellipsoid representation of complex **3**. The ellipsoids are drawn at 50% probability level.

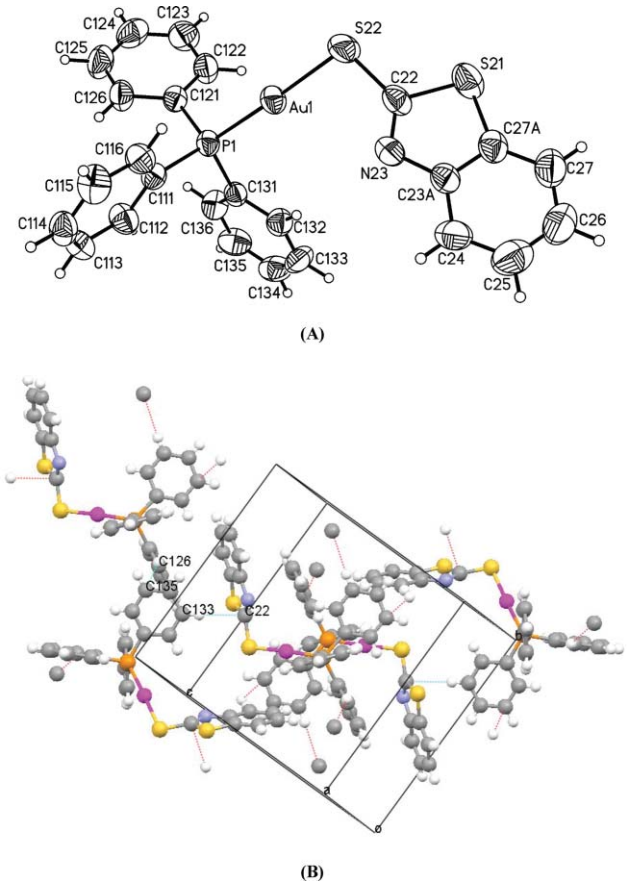

Fig. 4 (A) Anisotropic ellipsoid representation of complex **6**. The ellipsoids are drawn at 50% probability level. (B) Packing diagram of **6** with short contacts.

desulfurated thioamide counter part. The Au-Cl bond distances of 2.28-2.29 Å agree with those found in other $[AuCl_4^-]$ anions (2.27-2.28 Å in $[C_6H_{11}N_2][AuCl_4]$ ($[C_6H_{11}N_2]^+$=1-ethyl-3-methylimidazolium),[23a] 2.27-2.29 Å in $[C_8H_{15}N_2][AuCl_4]$ ($C_8H_{15}N_2]^+$= 1-butyl-3-methylimidazolium)[23a] and average 2.29 Å in $[C_1SCNmim][AuCl_4]$ ($C_1SCNmim$= 1-thiocyanomethyl-3-methylimidazolium chloride).[23b] The C-N bond distances in the desulfurated counter parts of complexes **1** and **2** are C1-N1= 1.308(7) Å and C7-N1= 1.398(6) Å (**1**) and C1-N2= 1.322(7) Å and C3-N2= 1.389(6) Å (**2**) respectively indicating that nitrogen participates in a partial double bond.[17,19] Moreover the angles around the C1 atoms were H1-C1-N1= 122.8°, H1-C1-S1= 122.8° and S1-C1-N1= 114.4 (4)° in **1** and H1-C1-N2= 124.9°, H1-C1-N1= 124.8° and N1-C1-N2= 110.4(4)° in **2** indicating sp^2 hybridization of the C atom confirming the existence of a double bond character between C and protonated N atoms in both complexes (Scheme 3).

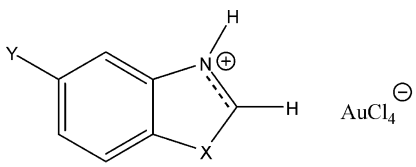

X= S and Y= H (**1**) or X= NH and Y= EtO (**2**)

Scheme 3

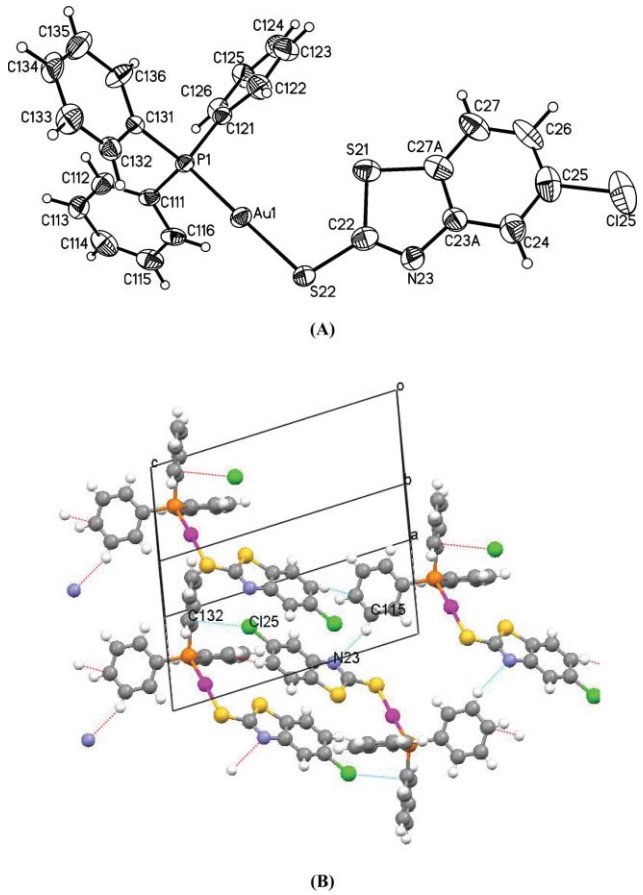

Fig. 5 (A) Anisotropic ellipsoid representation of complex **7**. The ellipsoids are drawn at 50% probability level. (B) Packing diagram of **7** with the short contacts.

Hydrogen bonding interactions N1[H1A]$\cdots$Cl$_2^{i}$= 3.257(4) Å (**1**) and N2[H2]$\cdots$Cl3^{ii}= 3.050(5) Å (**2**) (symmetry transformations: (i) –x+1/2, y–1/2, z and (ii) x, y, z+1) stabilize the supramolecular assemblies of complexes **1** and **2** (Figs. 1B and 2B).

Compound **3** is a zwitterion. The C-S bond distance is 1.808(3) Å indicating a single C-S bond while the C-N (1.34 Å) and C-C (1.39 Å) of the ring correspond to a delocalized double bond. The nitrogen atom is protonated resulting in a positive charge at N atom while the sulfonic group is negatively charged. The three S-O bond distances are almost equal with an average S-O bond length of 1.44 Å (Table 1) and they are in agreement with those found in the sulfonate group of $H_3O^+CF_3SO_3^-\cdot 4H_2O$ (average S-O distance of 1.444 Å).[24a] The S-O bond lengths of 1.437(3)-1.444(3) Å in **3** are shorter than the S-OH (1.56 Å) bond distance found in the sulfuric acid and closer to the S-O (1.43 Å) bond of the sulfuric acid,[24b] indicating partial double bond distribution and delocalization of the negative charge.

Natile *et al.*,[5] have previously described the mechanism of oxidation of diethyl-thioether to its oxo-derivative (Et_2SO) upon the reaction of Et_2S with $\{[AuCl_4]^-\}$ in acidic media[5] and proposed a mechanism, where the $\{[AuCl_4]^-\}$ was not the oxidation agent, but it was rather acting as a catalyst. Oxidation was caused by atmospheric di-oxygen which is simultaneously reduced to O^{2-}. These findings are confirmed here by the formation of complexes **1** and **2** and the isolation of compound **3**. Thus, in case of complexes **1** and **2**, the tetrachloroauronic anion is present in the complex as a counter anion since the desulfurated thione is protonated. The stability due to the charge delocalization in case of compound **3** leads to its isolation (see below). Therefore, a reasonable mechanism for the desulfuration of thione ligands could involve first the oxidation of thiones by di-oxygen, catalyzed by the presence of tetrachloroauric(III) anion followed by the C-S bond cleavage (in the cases of the ligands mbztH and EtmbzimH). In case of compound **3** the 2-sulfonate-nicotininc acid ($C_6H_5NO_5S$) is more stable than the other ligands, due to delocalization of the charge density, making the bond cleavage more difficult than in the other two ones. This is confirmed by the electrochemical and computational studies (see below). This indicates that both of the other two ligands produce similar intermediates, however ending up to **1** and **2** complexes, as less stable than **3**.

The reactions of **4** with the 2-mercapto-thiazolidine (mtzdH), 2-mercapto-benzothiazole (mbztH) and 5-chloro-2-mercapto-benzothiazole (ClmbztH) in the presence of potassium hydroxide produced mixed ligand complexes of formulae [Au(tpp)(mtzd)] (**5**), [Au(tpp)(mbzt)] (**6**) and [Au(tpp)(Clmbzt)] (**7**). One triphenyl-phosphine and one thioamide ligand are coordinated to Au(I) through their P and S atoms respectively. The geometry around Au(I) is linear with Au-P bond distances of 2.2960(13) Å (**6**) and 2.259(3) Å (**7**) respectively and Au-S bond lengths of 2.2961(13) Å (**6**) and 2.296(3) Å (**7**) respectively. The S-Au-P angle is almost 180° (176.25(5)°) for (**6**) and (176.11(9)°) for (7), respectively). The variation from 180° may be due to the packing of the molecules in the crystal lattice.Fig. 4B for (**6**): C133$\cdots$C22_e = 3.496(7), C126$\cdots$C135_f = 3.562(7) Å, Translation of Symmetry Code to Equiv. Pos: e = 3/2–x,1/2+y,–1/2–z, f = 3/2–x,–1/2+y,1/2–z (stacking interactions) and Fig. 5B for (**7**): Cl25$\cdots$C132_b = 3.369(13), N23$\cdots$C115_d = 3.355(19) Å, Translation of Symmetry Code to Equiv. Pos: b = 3–x,1–y,1–z, d= 3–x,1–y,2–z (hydrogen bondings).

Computational studies

The proposed desulfuration mechanism through the formation of a sulfonate intermediate derivative in the case of complexes **1** and **2** (Reaction IV), is further supported by PM6 calculations for the determination of the Bond Dissociation Energy of the C-SO_3H bond.

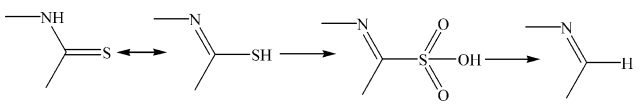

(IV)

The Bond Dissociation Enthalpies (BDE) for the C-S bond were obtained from the enthalpies of the different species using the expression: $BDE_{298}(R_1\text{-}R_2) = [\Delta_fH_{298}(R_1) + \Delta_fH_{298}(R_2)] - \Delta_fH_{298}(R_1\text{-}R_2)$ where (R_1-R_2) are the sulfur oxidized forms of the ligands, R_1 are the free ligands and R_2 the desulfurized forms of the ligands (See Scheme 2, Reaction II). Semi-empirical theoretical methods are especially designed to obtain enthalpy of formation of chemical systems with minimum computational cost and recent work has shown their reliability in BDE estimations.[25] PM6 gave the best results in our preliminary testing runs and therefore it was selected for the calculations. The calculated BDE values for the

Table 2 Electrochemical properties of complexes of **1-2** and **4-7** in acetonitrile[a]

	Oxidation potentials, (V)		Reduction potentials, (V)		
Compound	E^{I}_{p}	E^{II}_{p}	E^{I}_{p}	E^{II}_{p}	E^{III}_{p}
1	0.57[b]	1.15[b]	0.05	–0.51	–1.13
2	0.71[b]	1.34[b]	0.05	–0.51	–1.53
4	1.29		–1.79	—	—
5	0.93	—	–1.99		

[a] Peak potentials (V, *vs.* Ag/AgCl/KCl) were determined from cyclic voltammetric scans. Experimental conditions: Pt electrode, $v = 200$ mV/s, 293 K, acetonitrile containing 50 mM $TBABF_4$, E_p denotes peak potential of a chemically irreversible step. [b] In reverse anodic scan triggered beyond –0.5 V.

C-S bond (Reaction IV) of compound **3** is +310.16 kJ mol^{-1}, while the corresponding values for **1** and **2** are +148.16 and +111.96 kJ mol^{-1} respectively, indicating the easier formation of the desulfurated mbztH or EtmbzimH ligands in contrast to the desulfuration of the 2-sulfonate-nicotininc acid.

Electrochemical studies

(i) The complexes 1-2 and 4-7. The electrochemical behavior of **1-2** and **4-7** was studied in acetonitrile and DMF solutions, using cyclic voltammetry.[4b] The redox potentials of these complexes are summarized in Table 2. The cyclic voltammogram of the starting compound **4** displays one irreversible wave in acetonitrile controlled by diffusion (the dependence of I *vs.* $v^{1/2}$ has a linear character[26]) in the cathodic range at –1.79 V, which is in accordance with literature data and corresponds to the reduction of complex $RAuPPh_3$ with simultaneous formation of Au(0) and PPh_3.[27] In the anodic range the one-electron irreversible wave at 1.29 V was observed. Cyclic voltammograms of complex **5** show one irreversible cathodic wave. For the oxidative scan, an irreversible wave was observed.

The replacement of the Cl^- anion in complex **4** by a thioamide ligand with poorer electron-accepting ability as in the case of **5** leads to the increase in LUMO energy that results in Au(I)/Au(0) redox couple shift to a more negative potential as compared with complex **4**. For the anodic scan the one diffusion-controlled irreversible one-electron wave was observed at 0.93 V, which may be assigned to ligand oxidation as it has been shown previously for a series of $RAuPPh_3$.[27] This results to considerable shift of the metal-centered oxidation potential towards the anodic range and the corresponding metal-centered wave was not observed in the solvent's potential window. The electrochemical properties of complexes **6** and **7** were not studied in acetonitrile because of their poor solubility.

Cyclic voltammograms of complex **2** in acetonitrile are presented in Fig. 6(A). Three waves in the cathodic range of potentials were observed. The first one is irreversible and shows a diffusion character and corresponds to the transfer of two-electrons, *i.e.* the reduction process Au(III)→Au(I). The second one is a one-electron irreversible wave and the third one, at highest negative potential, is a one-electron irreversible one. Scheme 4 shows the steps of redox transformation of complex **2**. The first wave may be assigned to the reduction of complex **2** (step I at 0.05 V), that results to the destruction of the complex, thus forming $Au^{I}Cl$, Cl^- ions and the oxidized form of the ligand. The second wave at –0.51 V corresponds to the reduction of Au^{I} to Au^{0}. The third wave can be ligand-centered and shows reduction of the cationic

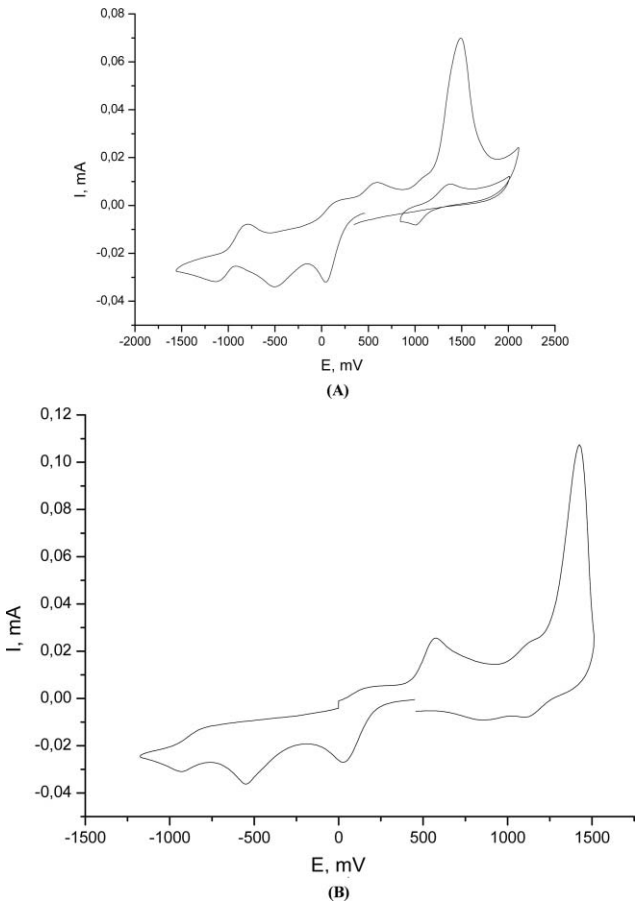

Fig. 6 Cyclic voltammograms of 1.1×10^{-3} M complexes **2** (A) and **1** (B) in CH_3CN. Experimental conditions: Pt working electrode, 50 mM $TBABF_4$, *vs.* Ag/AgCl/KCl, scan rate $v = 0.2$ V.

species to the radical one. After triggering the potential at –1.8 V the one-electron wave which appears, is assigned to the oxidation of a product formed during the reduction of **2**. In the anodic range the reverse scan shows three irreversible waves. The third one at 1.34 V is an one-electron wave and obviously corresponds to Cl^-/Cl^0 oxidation.[28] The nature of the first and second waves might be connected with some chemical reactions which take place in the reduction process of the complex.

The reverse scan after triggering the potential at $E < -0.5$ V generates the new peak at 1.4 V. The characteristic triangle form and a significant discordance between the concentration of the complex and the current value, indicate the adsorption character of this wave (Fig. 6A). We propose that this peak

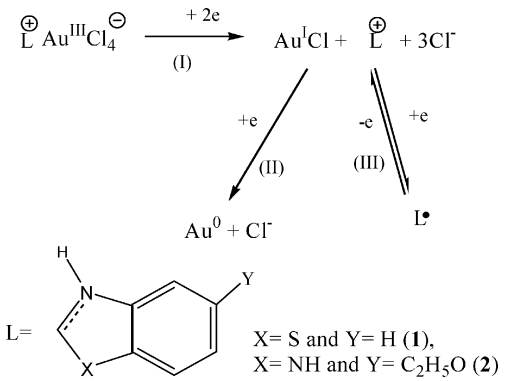

Scheme 4

corresponds to the oxidation of adsorbed Au^0 on the surface of the electrode.

The electrochemical behavior of complex **1** is similar to that of complex **2** and can also be explained by Scheme 4. In this case the potential of the third peak is shifted to more positive potentials compared with complex **2** ($\Delta E \approx 100$ mV, Table 2). The more negative reduction potential observed for the third reduction wave in the case of **2** could be readily rationalized by the presence of the electron-donating alkoxyl substituent in 2-mercaptobenzothiazole ligand, which makes it more electron-donor and poorer π-acceptor, and hence reduces its reduction potential. This fact also reinforces the assumption that the nature of this wave is assigned to the ligand reduction. Similar electrochemical behavior was observed in the electrochemical study of the complexes of Au(III) with 2,2′-bipyridine and oxygen containing ligands.[29] In cyclic voltammetric experiments, performed with a Pt-electrode in acetonitrile, cationic species containing the $Au(bipy)^{3+}$ moiety and additional oxygen-donor ligands, undergo two or three cathodic processes. Electroreduction by means of controlled potential electrolyses of all compounds studied, affords elemental gold identified by elemental analyses, free bipyridine ligand and Cl^- species (in the case of complexes with Cl-substituents). This fact may be considered as an additional evidence of the proposed reactions in Scheme 4, which is in agreement with the experimental results obtained.

Cyclic voltammograms of **5-7** in DMF exhibit one irreversible wave in the cathodic range and three one-electron diffusion-controlled irreversible waves at the anodic scan. A typical voltammetry curve is presented in Fig. 7. The values of the anodic and cathodic peak potentials are listed in Table 3.

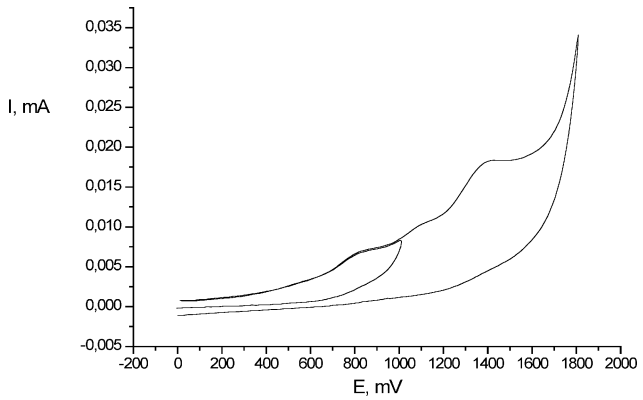

Fig. 7 Cyclic voltammetry curve for 1.1×10^{-3} M complex **7** in DMF. Experimental conditions: Pt working electrode, 50 mM $TBABF_4$, *vs.* Ag/AgCl/KCl, scan rate $v = 0.2$ V/s.

It should be noted that the presence of the electron-accepting Cl substituents in the 2-mercaptobenzothiazole ring results in the shift of peak potentials to more positive values (Table 3). It was shown previously,[27] that the oxidation of complexes Ph_3PAuR (R = Me, Ph, MeO, Cl, Br, I) in acetonitrile proceeds through the formation of the $Ph_3PAuR^{+\bullet}$ radical-cation. Decomposition of these species leads to unstable compounds RAu and the formation of Au(0) and R, as described in ref. 26. In the case of Ph_3PAuCl (**4**) no distinct waves in the anodic range appear within the limits of the solvent potential window (at ≈ 1.6 V the discharge of solvent molecules begins). In the cathodic scan the one-electron diffusion-controlled the irreversible wave was observed at –0.59 V.

The electrochemical behavior of complexes **1**, **2** and **4** in DMF is very similar to the one in acetonitrile: three irreversible waves in the cathodic range were observed. Therefore, the reduction of these compounds may be described as in Scheme 4.

(ii) The ligand. The redox properties of the ligands EtmbzimH, mbztH and $mnaH_2$ were studied in an attempt to contribute to the elucidation of the mechanism of the desulfuration process, caused by Au(III) ions. As follows from cyclic voltammograms (Fig. 8), all ligands display the irreversible one-electron wave, controlled by diffusion at anodic range of potentials. The irreversibility takes place in the range of scan rate from 50 mV/s to

Table 3 Electrochemical properties of complexes of **1-2** and **4-7** in DMF[a]

	Oxidation potentials, (V)			Reduction potentials, (V)		
Compound	E^I_p	E^{II}_p	E^{III}_p	E^I_p	E^{II}_p	E^{III}_p
1	0.65	1.44	—	-0.66	-0.93	-1.76
2	—	1.35		-0.68	-0.95	—
4	—	—	—	-0.59	—	—
5	0.72	1.1	1.42	-0.68	—	—
6	0.68	1.05	1.32	-0.83	—	—
7	0.82	1.12	1.44	-0.90	—	—

[a] Peak potentials (V, *vs.* Ag/AgCl/KCl) were determined from cyclic voltammetric scans. Experimental conditions: Pt electrode, $v = 200$ mV/s, 293 K, acetonitrile containing 50 mM $TBABF_4$, E_p denotes peak potential of a chemically irreversible step.

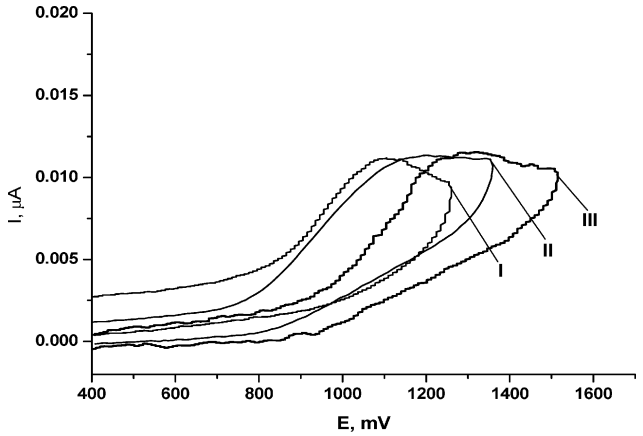

Fig. 8 Cyclic voltammograms of ligands: EtmbzimH (I); mbztH (II); mnaHz (III) (CH_3CN, 100 mV/s; Pt; 10^{-3} M; Ag/AgCl/HCl).

1000 mV/s that is typical for an EC mechanism (electrochemical-chemical mechanism). The peak potentials are in good agreement with the well-known literature data and may be assigned to the SH-group oxidation.[28]

This fact points out that these compounds exist in tautomeric forms in acetonitrile solutions and the equilibrium is shifted to the SH-containing form as the oxidation proceeds (Scheme 5):

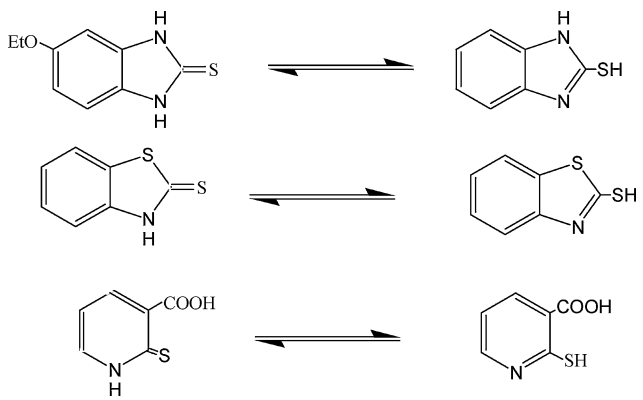

Scheme 5

The values of the anodic peak potentials are listed in Table 4. The easiness of ligand's oxidation changes in the order: EtmbzimH > mbztH > $mnaH_2$ which correlates with the electronic effects of substituents in benzene ring. The change of the ethoxy-group for a H-atom in mbztH results to the shift of the potential to more positive values. The $mnaH_2$ ligand oxidizes most hardly due to the strong presence of the strong electron withdrawing carboxy group.

The first step of $HAuCl_4$ reaction with these ligands (as well as electrochemical oxidation) might be the oxidation of the SH-group followed by desulfuration (Reaction II). Since in the case of $mnaH_2$ only the oxidized derivative was isolated and characterized, we made an attempt to obtain the desulfurated product by means of the controlled potential electrolyses which was performed in acetonitrile at the first anodic wave potential of E= 1.3 V. In the NMR-spectrum of the product, the proton signal of the SH-group disappeared after electrolyses. The signal of the carboxy group proton on the other hand, was shifted to lower fields and a widening was observed, obviously, because of hydrogen bond formation between the carboxy and sulfo groups. These facts support the assumption that the oxidation of $mnaH_2$ ligand proceeds the desulfuration step.

Table 4 Electrochemical properties of the ligands EtmbzimH, mbztH and mnaH2 in acetonitrile (Pt, 200 mV/s, 293 K, acetonitrile containing 50 mM $TBABF_4$ V, *vs.* Ag/AgCl/KCl)

Ligand	E_{ox}, V
EtmbzimH	1.02
mbztH	1.17
mnaH2	1.3

Biological tests

Complexes **1-2** and **4-7** and $HAuCl_4$ were tested for cytotoxic activity against leiomyosarcoma cells from the Wistar rat, polycyclic aromatic hydrocarbons (PAH, benzo[a]pyrene) carcinogenesis. Cytotoxic activities for complexes **1-2** and **4-7** and $HAuCl_4$ were evaluated as percentage of cells surviving after being exposed to multiple concentrations of a test compound for 24 h time period. The IC_{50} values after treatment for 24 h were 1.3 ± 0.9 (**1**), 0.7 ± 0.1 (**2**), inactive (**4**), 0.8 ± 0.4 (**5**), 2.1 ± 1.3 (**6**) and 1.1 ± 0.5 (**7**) μM respectively, while $HAuCl_4$ was found to be inactive against leiomyosarcoma cells (IC_{50}= 4-5 μM[6]), for cisplatin. Consequently, complexes **2** and **5**, containing Au(III) and Au(I) respectively, were the more active among **1-2** and **4-7**. The IC_{50} values of these complexes, cisplatin and other metals, against leiomyosarcoma cells are compared in Table 5. Gold complexes **2** and **5**, are less active than the tin complexes {$(Ph_3Sn)_2$(MNA)(Me_2CO)} and Ph_3Sn(PMT) with IC_{50} values 0.005 and 0.1 μM respectively but they show comparable activity with that of silver(I) complexes (Table 5). Among complexes of the same ligand 5-chloro-2-mercapto-benzothiazole, (**7**, $Me_2Sn(CMBZT)_2$, (n-$Bu)_2Sn(CMBZT)_2$, $Ph_2Sn(CMBZT)_2$ and Ph_3Sn(CMBZT)) the diorganotin complex $Ph_2Sn(CMBZT)_2$ show higher activity and the same order is followed between gold(I) and organotin complexes **6** and Ph_3Sn(MBZT) of 2-mercapto-benzothiazole ligand (Table 5).

Conclusions

Based on crystallographic and computational results a possible mechanism for the desulfuration of thioamide ligands upon their reaction with {$[AuCl_4]^-$} ions was proposed.

The isolation of the stable enough compound **3** and the final desulfurated complexes **1** and **2** strongly indicate that the $AuCl_4^-$ ions, which catalyzes the oxidation of S to $-SO_3^-$ by atmospheric O_2, regenerates and acts as a counter ion in **1** and **2**. Both electrochemical and computational results indicate that the oxidation of S takes place prior to C-S breakage and desulfuration and justifies the stability of **3**, as compared to the sulfonate derivatives of the other ligands.

The catalytic role of $AuCl_4^-$ in the oxidation of thioethers by atmospheric O_2 had also been proposed earlier by Natile *et al.*[5] Au(III) is most probably first reduced to Au(I) and re-oxidized back to Au(III). This is the case of the electrochemical behavior of the complexes in this study, where a two electron process for the reduction of Au(III) to Au(I) was detected. It should be noted however, that kinetic data would be required to allow a more definitive conclusion on any proposed mechanism, to be made.

Table 5 Cytotoxic activity of Au(III)/(I), Ag(I) and Sn complexes as IC_{50} (μM) values against leiomyosarcoma cells[6]

Complex	50% inhibitory concentration (IC_{50}) (μM)
Cisplatin	4-5
1	1.3 ± 0.9
2	0.7 ± 0.1
4	inactive
5	0.8 ± 0.4
6	2.1 ± 1.3
7	1.1 ± 0.5
$\{[AgCl(TPTP)]_4\}^a$	0.8
$[AgCl(TPTP)_3]^a$	0.7
$[AgBr(TPTP)_3]^a$	0.8
$[AgI(TPTP)_3]^a$	0.9
$Me_2Sn(CMBZT)_2{}^b$	5-7.5
$(n\text{-}Bu)_2Sn(CMBZT)_2{}^b$	0.6-0.8
$Ph_2Sn(CMBZT)_2{}^b$	0.3-0.5
$Ph_3Sn(CMBZT)^b$	0.5-0.8
$Me_2Sn(PMT)_2{}^c$	20-60
$(n\text{-}Bu)_2Sn(PMT)_2{}^c$	0.7
$Ph_2Sn(PMT)_2{}^c$	1-2
$Ph_3Sn(PMT)^c$	0.1
$Ph_3Sn(MBZO)^d$	1.3-3
$Ph_3Sn(MBZT)^e$	1.5-3
$\{(Ph_3Sn)_2(MNA)(Me_2CO)\}^f$	0.005
$[SbBr_3(TU)_2]^g$	23.5 (unpublished results)

[a] TPTP = tri(p-toly)phosphine. [b] CMBZTH = 5-chloro-2-mercapto-benzothiazole. [c] PMTH = 2-mercapto-pyrimidine. [d] MBZOH = 2-mercapto-benzoxazole. [e] MBZT = 2-mercapto-benzothiazole. [f] H_2MNA = 2-mercapto-nicotinic acid. [g] TU = thiourea.

The formation of the mixed ligand gold(I) complexes of formulae [Au(tpp)(mtzd)] (**5**), [Au(tpp)(mbzt)] (**6**) and [Au(tpp)(Clmbzt)] (**7**) where no desulfuration of the ligands takes place emphasizes the possible catalytic role of $AuCl_4^-$ in the oxidation and desulfuration of the ligands.

Finally, complexes **2** and **5** containing Au(III) and Au(I) showed the higher *in vitro* cytotoxicity against leiomyosarcoma cells, although there is no significant differences on the cytotoxic profile between the complexes **1**, **2**, **5**, and **7**. These complexes were also found more active than *cis*-Pt. Complexes **2** and **5** exhibit lower activity than the corresponding $\{(Ph_3Sn)_2(MNA)\ (Me_2CO)\}$ and $Ph_3Sn(PMT)$ complexes, while they show comparable activity with that of silver(I) complexes (Table 5). Among gold and organotin complexes of the same ligand, tin complexes are again more active.

Experimental

Materials and instruments

All solvents used were of reagent grade, while thioamides and triphenyl-phosphine (Aldrich, Merk) were used with no further purification. The tetrachloroauric(III) acid ($HAuCl_4$) solution (0.51 M) was prepared by dissolving 1 g Au foil into 10 ml mixture of concentrated hydrochloric acid (12 M) and nitric acid (16 M) 4:1.[7] Elemental analyses for C, H, N, and S were carried out with a Carlo Erba EA MODEL 1108 elemental analyzer. Infra-red spectra in the region of 4000-370 cm^{-1} were obtained in KBr discs. Far-infra-red spectra in the region of 400-50 cm^{-1} were obtained in polyethylene discs, with a Perkin-Elmer Spectrum GX FT-IR spectrophotometer. A Jasco Uv/Vis/NIR V 570 series spectrophotometer was used to obtain the electronic absorption spectra. The ^{1}H-NMR spectra were recorded on a Bruker AC 250, 400 MHFT-NMR instrument in $CDCl_3$ or DMSO-d_6 solutions. Chemical shifts δ are given in ppm using ^{1}H-TMS as internal reference. Micro Raman spectra (64 scans) were recorded at room temperature using a low power (~30 mW) green (514.5) mm laser on a Renishaw In Via spectrometer set at 2.0 resolution. Thermal studies were carried out on a Shimadzu DTG-60 simultaneous DTA-TG apparatus, under a N_2 flow (50 cm^3 min^{-1}) at a heating rate of 10 °C min^{-1}.

Synthesis of compounds $\{[AuCl_4]^-[bztH_2]^+\}$ (1), $\{[AuCl_4]^-[EtbzimH_2]^+(H_2O)\}$ (2), the 2-sulfonate-nicotininc acid (3), [Au(tpp)(mbzt)] (6) and [Au(tpp)(Clmbzt)] (7)

Complexes **1** and **2** were synthesized as follows: 1 mmol of the appropriate thioamide ligand (0.167 g 2-mercapto-benzothiazole and 0.194 g of 5-ethoxy-2-mercapto-benzimidazole) were dissolved in 10 ml methanol. 10 ml acetonitrile solution which contains 0.5 mmol $HAuCl_4$ 1 ml (0.51 M) was then added to the ligand's methanolic solution. The resulting solution was heated for 3 hours under reflux. After cooling the solution was filtered off. Slow evaporation of the resulting clear solution form crystals of complexes **1** and **2** suitable for X-ray analysis. Crystals of compound **3** were obtained derived by slow evaporation of the solution resulted from mixing 10 ml acetonitrile solution of 0.5 mmol $HAuCl_4$ 1 ml (0.51 M) with 10 ml methanolic solution of 1 mmol of 2-mercapto-nicotinic acid (0.155 g) in the presence of 1 mmol KOH (1 ml, 1 N).

The precursor [Au(tpp)Cl] (**4**) was derived from the reaction between 1 mmol tri-phenyl-phosphine (0.262 g) with 0.5 mmol of $HAuCl_4$ solution (1 ml, 0.5 M) in 10 ml methanol.[5b] Crystals of complex **4** were grown from a 20 ml dichloromethane solution. Complexes **5**, **6** and **7** were synthesized as follows: A suspension of 0.215 mmol of the appropriate thioamide (0.026 g 2-mercapto-thiazoline for **5**, 0.034 g 2-mercapto-benzothiazole for **6** and 0.042 g 5-chloro-2-mercapto-benzimidazole for **7**) in distilled water (5 ml) was treated with a solution of KOH 1 N (1 cm^{-3}, 1 mmol). The resulting clear solution was then added to 5 ml of a methanolic solution of 0.215 mmol [Au(tpp)Cl] (0.106 g) under stirring for 2 hours. The white precipitate was then filtered off and dried. Crystals of complexes **5**, **6** and **7** suitable for X-ray analysis were formed from slow evaporation of a dichloromethane/toluene solution (1:1) of the above powders.

[**1**] Yield 31%. m.p. 232-240 °C. Found: C, 17.89%; H, 1.08%; N, 2.63%; S, 6.68%. Calc. for $C_7H_8NOSAuCl_4$: C, 17.70%; H, 1.27%; N, 2.95%; S, 6.75%. IR (KBr): 3440.00 w, 3208.88 w, 3072.67, 1458.88, 1404.86 m, 1270.38, 766.01 s, 700.21 s. ^{1}H NMR (DMSO-d_6) δ 9.34 s, H(NH); 8.12 s, H(CH);; 8.03 m, H(Ar); 7.48 m, H(Ar). ESI-MS(+): *m/z* 663, 573, 484, 323, 268, 163. ESI-MS(–): *m/z* 339.

[**2**] Yield 54%. m.p. 165-170 °C. Found: C, 21.34%; H, 2.72%; N, 5.14%. Calc. for $C_9H_{13}N_2O_2AuCl_4$: C, 20.79%; H, 2.52%; N, 5.39%. IR (KBr): 3568.88, 3280.00 w, 3130.85 *vs*, 2955.55 m, 1631.63 s, 1512.53, 1446.53 s, 1348.00, 1294.57 s, 1261.51, 1187.17 s, 1106.27, 1040.60, 815.47 s, 591.76. Far-IR (Polyethylene): 362.12 *vs*, 239.59 s, 147.78 s, 135.97 s, 89.37 s, 56.99 s. ^{1}H NMR (DMSO-d_6) δ 9.31 s, H(NH); 8.28 s, H(CH); 7.69 m, H(Ar); 7.15 m, H(Ar); 4.08 m, H(CH_2O); 1.34, H(CH_3). ESI-MS(+): *m/z* 663, 573, 323, 268, 136. ESI-MS(–): *m/z* 339.

[**4**] Yield 76%. m.p. 236-240 °C. Found: C, 43.14%; H, 2.98%. Calc. for $C_{18}H_{18}AuPCl$: C, 43.70%; H, 3.06%. IR (KBr): 3433.22 w,

3053.33, 1479.10, 1435.44 s, 1179.39, 1101.89 s, 998.65, 748.00 s, 712.70, 692.90 *vs*, 546.65 s, 502.31 s. Far-IR (Polyethylene): 330.12 *vs*, 171.89 s. ^{1}H NMR ($CDCl_3$) δ 7.55 m, H(Ar).

[**5**] Yield 74%. m.p. 160-161 °C. Found: C, 43.98%; H, 3.26%; N, 2.64%; S, 10.91%. Calc. for $C_{21}H_{17}AuNPS_2$: C, 43.83%; H, 2.98%; N, 2.43%; S, 11.14%. IR (KBr): 3053.33, 2915.55 m, 1554.96 *vs*, 1478.99, 1435.57 *vs*, 1303.02, 1181.67, 1100.53 s, 1022.00, 996.65 s, 963.11 s, 917.49 s, 750.24 s, 709.30, 692.08 *vs*, 631.68, 538.10 *vs*, 502.53 s. Far-IR (Polyethylene): 279.29 *vs*, 245.94 s, 151.08 s, 179.64, 99.43 *vs*, 75.48 *vs.* ^{1}H NMR ($CDCl_3$) δ 7.50 m, H(Ar(Ph_3P)); 4.28 m H4(CH_2), 3.38 m, H5(CH_2). ESI-MS(+): *m/z* 1036, 721, 600, 578, 573.

[**6**] Yield 80%. m.p. 157-161 °C. Found: C, 48.33%; H, 3.18%; N, 2.39%; S, 9.90%. Calc. for $C_{25}H_{19}AuNPS_2$: C, 48.00%; H, 3.06%; N, 2.24%; S, 10.25%. IR (KBr): 3048.88, 1478.62, 1433.85 s, 1417.03 *vs*, 1308.59, 1272.59, 1234.89, 1099.85 s, 1073.00, 993.17, 971.66 *vs*, 757.12 s, 709.30, 691. 50 *vs*, 538.59 *vs*, 501.65 s.%. Far-IR (Polyethylene): 279.94 s, 178.48, 89.30 m, 38.95 *vs.*^{1}H NMR ($CDCl_3$) δ 7.60 m, H(Ar(Ph_3P)); 7.25 m, H(Ar(BZT)). ESI-MS(+): *m/z* 1084, 721, 626, 648, 573.

[**7**] Yield 86%. m.p. 88-91 °C. Found: C, 45.33%; H, 2.98%; N, 2.13%; S, 9.74%. Calc. for $C_{25}H_{18}AuNClPS_2$: C, 45.50%; H, 2.75%; N, 2.12%; S, 9.72%. IR (KBr): 3051.54, 1479.24, 1435.50 s, 1408.97 *vs*, 1308.08 m, 1101.22 s, 1065.82, 998.38 *vs*, 790.99, 750.13 s, 693.40 *vs*, 537.85 s, 503.93 s. Far-IR (Polyethylene): v 279.11 s, 170.88 s, 88.85 s, 70.09 s, 54.29 s. ^{1}H NMR ($CDCl_3$) δ 7.56 m, H(Ar(Ph_3P)); 7.14 m, H(Ar(CBZT)). ESI-MS(+): *m/z* 1118, 721, 682, 660, 573.

Crystallography

Intensity data for the crystals of **1** were collected on a Bruker KappaCCD diffractometer and for **2** on a Bruker APEXII CCD diffractometer, both at the windows of a Bruker FR591 rotating anode (ϕ scans and ω scans to fill the asymmetric unit) in the range 3.1°–27.5° for **1** and 3.2°–27.5° for **2**, using graphite-monochromated MoK_α radiation (λ = 0.71073 Å) at 120(2) K, controlled by the COLLECT software package.[30] The data were processed by DENZO[31] and corrected for absorption by using SADABS.[32] The structures were solved using SIR92[33] (**1**) and SIR2004 (**2**)[34] and refined using SHELXL-97.[35] All non-hydrogen atoms were refined anisotropically with hydrogen atoms included in idealized positions and refined using a riding model. Each formula unit of **2** contains in total five water molecules, one of which is disordered and one disordered molecule of $[H_3O]^+$. There are also four chloride ions. The presence of the $[H_3O]^+$ molecule means that the charge in the formula unit is balanced. It was only possible to locate hydrogen atoms for one of the water moieties, O2. For all other water molecules and the $[H_3O]^+$ molecule it was found impossible to locate the hydrogen atoms because of the use of X-ray radiation, the presence of the very heavy gold atom and the low occupancies of water at these positions. For this reason it is not possible to assign which of the O4 and O5 atoms belongs to a water molecule and which belongs to the acid, as the assignment of either atom as the acid would give the correct charge balance. It is highly probable that the O3, O4 and O5 moieties are involved in hydrogen bonding, but this is impossible to confirm due to the fact that the hydrogen atoms in these moieties could not be located.

Intensity data for the crystals of **3**, **4** and **5** were collected on Bruker P4 diffractometer, with graphite monochromatized MoKa radiation (λ = 0.71073 Å) at 293(2) K. The structures were solved with SHELXS-97[36] and refined with SHELXL-97.[35] All non-hydrogen atoms were refined anisotropically. Hydrogen atoms were located by difference maps and refined isotropically.

Intensity data for the crystals of **6** and **7** were collected on KUMA KM4CCD four-circle diffractometer[37] with CCD detector, using graphite-monochromated MoKα (λ = 0.71073 Å). Cell parameters were determined by a least-squares fit.[38] All data were corrected for Lorentz-polarization effects and absorption.[38,34]

In these gold structures, the large residual electron density peaks observed are due to the high atomic radius of gold atom.

The structure was solved with direct methods with SHELXS97[36] and refined by full-matrix least-squares procedures on F^2 with SHELXL97.[35] All non-hydrogen atoms were refined anisotropically, hydrogen atoms were located at calculated positions and refined with 'riding model' with isotropic thermal parameters fixed at 1.2 times the U_{eq}'s of appropriate carrier atom.

Significant crystal data are given in Table 6.

Table 6 Crystal data and the structure refinement details of the compounds

	1	**2**	**3**	**6**	**7**
Empirical formula	$C_7H_6AuCl_4NS$	$C_{36}H_{53}AuCl_8N_8O_{10}$	$C_6H_5NO_5S$	$C_{25}H_{19}AuNPS_2$	$C_25H_{18}AuClNS_2$
Fw	474.95	1238.43	203.18	625.49	634.26
Temperature (K)	120(2)	120(2)	293(2)	293(2)	293(2)
Cryst. System	Orthorhombic	Monoclinic	Triclinic	Monoclinic	Triclinic
Space group	*Pbca*	*C*2/*m*	*P*-1	$P2_1/n$	*P*-1
a, Å	15.3524(4)	22.0808(5)	6.762(1)	12.7430(9)	8.8981(4)
b, Å	7.7452(2	25.1431(7)	7.840(1)	12.9378(7)	11.0221(4)
c, Å	19.3505(3)	4.8774(1)	8.797(1)	13.6063(6)	14.1845(6)
α, deg	90	90	63.61(1)	90	89.145(3)
β, deg	90	92.500(2)	85.35(1)	95.993(5)	76.610(4)
γ, deg	90	90	65.39(1)	90	83.837(4)
V, Å^3	2300.92(9)	2705.26(11)	376.71(10)	2231.0(2)	1345.45(10)
Z	8	2	2	4	2
ρ_{calcd}, g cm^{-3}	2.742	1.520	1.791	1.862	1.629
μ, mm^{-1}	13.855	3.168	3.826	6.866	5.793
Data Collected	27049	15931	1670	27267	9926
Independent Reflections (Rint)	2623 (0.058)	3171 (0.048)	1358 (0.101)	5080 (0.028)	4736 (0.056)
R1, wR2 [I>2σ(I)]	0.027, 0.0575	0.043, 0.1054	0.055, 0.1502	0.026, 0.0666	0.068, 0.2069

Computational studies

The ground state optimizations on the investigated molecules were carried out without any constraints using the PM6 semiempirical method[39] as this is implemented in MOPAC 2007 program,[40] utilizing the eigenvector following algorithm.[41]

Electrochemical study

All electrochemical measurements were carried out under argon at room temperature. Cyclic voltammetry experiments were performed in classical three-electrode cell in CH_3CN solution with 0.05 M $TBABF_4$ as supporting electrolyte using a model IPC-Win potentiostat. The number of electrons transferred were determined by comparing with the height of Fc^{2+}/Fc^{3+} =0.45 V wave for the same concentration and coulometrically. A platinum working electrode with diameter 2 mm, platinum wire auxiliary electrode and aqueous Ag/AgCl/KCl (sat.) reference electrode were used. The solvents were routinely distilled and dried prior to use.

Biological tests

These have been described in detail elsewhere.[42]

Acknowledgements

This research was carried out in partial fulfilment of the requirements for the master thesis of K.N.K. under the supervision of S.K.H., within the graduate program in Bioinorganic Chemistry. S.K.H., E.R.M. and N.H. would like to thank a NATO grant for the exchange of scientists. E.R.M. also thanks RFBR grant N09-03-00743

References

1 *Martidale The Extra Pharmacopoeia*, 28th ed.; J. E. F. Raynolds, Ed.; The Pharmaceutical Press: London, 1982.
2 S. Miranda, E. Vergara, F. Mohr, D. de Vos, E. Cerrada, A. Mendía and M. Laguna, *Inorg. Chem.*, 2008, **47**, 5641–5648.
3 J. Zou, P. Taylor, J. Dornan, S. P. Robinson, M. D. Walkinshaw and P. J. Sadler, *Angew. Chem., Int. Ed.*, 2000, **39**, 2931–31.
4 (*a*) E. R. T. Tiekink, *Crit. Rev. Oncol. Hematol.*, 2002, **42**, 225–248; (*b*) L. Ronconi, L. Giovagnini, C. Marzano, F. Bettìo, R. Graziani, G. Pilloni and D. Fregona, *Inorg. Chem.*, 2005, **44**, 1867–1881.
5 G. Annibale, L. Canovese, L. Cattalini and G. Natile, *J. Chem. Soc., Dalton Trans.*, 1980, 1017–1021.
6 S. K. Hadjikakou, I. I. Ozturk, M. N. Xanthopoulou, P. C. Zachariadis, S. Zartilas, S. Karkabounas and N. Hadjiliadis, *J. Inorg. Biochem.*, 2008, **102**, 1007–1015, and references therein.
7 B. P. Block, *Inorg. Synth.*, 1953, **4**, 14.
8 A. K. Al-Sa'ady, C. A. McAuliffe, R. V. Parish and J. A. Sandbank, *Inorg. Synth.*, 1985, **23**, 191–194.
9 N. C. Baenziger, W. E. Bennett and D. M. Soboroff, *Acta Crystallogr.*, 1976, **32**, 962–963.
10 M. Khan, C. Oldham and D. G. Tuck, *Can. J. Chem.*, 1981, **59**, 2714–2718.
11 T. A. Grant, J. M. Forward and J. P. Fackler, *Z. Kristallogr.*, 1996, **211**, 483.
12 U. E. I. Horvath, S. Cronje, S. D. Nogai and H. G. Raubenheimer, *Acta Crystallogr., Sect. E: Struct. Rep. Online*, 2006, **62**, m1644.
13 N. Hadjililiadis and T. Theophanides, *Can. J. Spectroscopy.*, 1971, **16**, 135.
14 N. Hadjiliadis, A. Yannopoulos and R. Bau, *Inorg. Chim. Acta*, 1983, **69**, 109–115.
15 P. C. Zachariadis, S. K. Hadjikakou, N. Hadjiliadis, A. Michaelides, S. Skoulika, Y. Ming and Y. Xiaolin, *Inorg. Chim. Acta*, 2003, **343**, 361–365.
16 G. J. Corban, S. K. Hadjikakou, N. Hadjiliadis, M. Kubicki, E. R. T. Tiekink, I. S. Butler, E. Drougas and A. M. Kosmas, *Inorg. Chem.*, 2005, **44**, 8617–8627.
17 V. Daga, S. K. Hadjikakou, N. Hadjiliadis, M. Kubicki, J. H. Z. Santos and I. S. Butler, *Eur. J. Inorg. Chem.*, 2002, 1718–1728.
18 S. K. Hadjikakou, P. Aslanidis, P. Karagiannidis, D. Mentzafos and A. Terzis, *Inorg. Chim. Acta*, 1991, **186**, 199–204.
19 (*a*) I. I. Ozturk, S. K. Hadjikakou, N. Hadjiliadis, N. Kourkoumelis, M. Kubicki, M. Baril, I. S. Butler and Jan Balzarini, *Inorg. Chem.*, 2007, **46**, 8652–8661; (*b*) M. N. Xanthopoulou, S. K. Hadjikakou, N. Hadjiliadis, M. Kubicki, S. Skoulika, T. Bakas, M. Baril and Ian S. Butler, *Inorg. Chem.*, 2007, **46**, 1187–1195.
20 E. A. Allen and W. Wilkinson, *Spectrochim. Acta*, 1972, **2**, 2257–2262.
21 I. S. Butler, A. Neppel, K. R. Plowman and C. F. Shaw, *J. Raman Spectrosc.*, 1984, **15**, 310.
22 A. G. Jones and D. B. Powell, *Spectrochim. Acta*, **30**, 563–570.
23 (*a*) M. Hasan, I. V. Kozhevnikov, M. R. H. Siddiqui, A. Steiner and N. Winterton, *Inorg. Chem.*, 1999, **38**, 5637; (*b*) D. Zhao, Z. Fei, W. H. Ang, R. Scopelliti and P. J. Dyson, *Eur. J. Inorg. Chem.*, 2007, 279–284.
24 (*a*) J.-O. Lundgren, *Acta Crystallogr., Sect. B: Struct. Crystallogr. Cryst. Chem.*, 1978, **34**, 2432–2435; (*b*) C. E. Housecroft, A. G. Sharpe, *Inorganic Chemistry* 3nd edition, Pearson Education, Paperback, 2007, chapter 16, page 523.
25 T. Nishiyama, S. Shiotsu, H. Tsujita, *Polymer Degradation and Stability*, 2002, 76, 435-439.
26 K. P. Butin, R. D. Rachimov, V. P. Dyadchenko and O. A. Enyukova, *Memalloorganicheskaya khimia*, 1989, **2**, 1401–1404.
27 J. Heinze, *Angew. Chem., Int. Ed. Engl.*, 1984, **23**, 831–918.
28 Ch. Mann and K. Barnes, *Electrochemical reactions in nonaqueous systems*, Marcel Dekker, Inc., New York, 1970.
29 G. Sanna, M. I. Pilo, G. Minghetti, M. A. Cinellu, N. Spano and R. Seeber, *Inorg. Chim. Acta*, 2000, **310**, 34.
30 R. Hooft and B. V. Nonius, Data collection software, 1998.
31 Z. Otwinowski, W. Minor, *Methods in Enzymology*, 1997 Vol. 276: *Macromolecular Crystallography*, part A, pp. 307-326; C. W. Carter, Jr. & R. M. Sweet, Eds., Academic Press.
32 G. M. Sheldrick, *SADABS - Bruker Nonius area detector scaling and absorption correction - V2.10*.
33 A. Altomare, G. Cascarano, C. Giacovazzo and A. Guagliardi, *J. Appl. Crystallogr.*, 1993, **26**, 343–350.
34 M. C. Burla, R. Caliandro, M. Camalli, B. Carrozzini, G. L. Cascarano, L. De Caro, C. Giacovazzo, G. Polidori and R. Spagna, *J. Appl. Crystallogr.*, 2005, **38**, 381–388.
35 G. M. Sheldrick, *SHELXL-97, Program for refinement of crystal structures*, University of Göttingen, Germany, 1997.
36 G. M. Sheldrick, *SHELXS-97, Program for solution of crystal structures*, University of Göttingen, Germany, 1997.
37 *CrysAlisCCD* (Version 1.171.29.9) Oxford Diffraction, Wrocław, Poland, 2006.
38 *CrysAlisRED* (Version 1.171.29.9). Oxford Diffraction, Wrocław, Poland, 2006.
39 J. J. P. Stewart, *J. Mol,. Mod.*, 2007, 13, 1173–1213.
40 J. J. P. Stewart, *MOPAC* 2007, Stewart Computational Chemistry, Colorado Springs, CO, USA, http://OpenMOPAC.net.
41 J. Baker, *J. Comput. Chem.*, 1986, **7**, 385.
42 M. N. Xanthopoulou, S. K. Hadjikakou, N. Hadjiliadis, E. R. Milaeva, J. A. Gracheva, V.-Y. Tyurin, N. Kourkoumelis, K. C. Christoforidis, A. K. Metsios, S. Karkabounas and K. Charalabopoulos, *Eur. J. Med. Chem.*, 2008, **43**, 327.

